ChemPubSoc Europe

DOI: 10.1002/chem.201405369

CHEMISTRY
A European Journal
Full Paper

Polyoxometalates

New Polyoxometalates Containing Hybrid Polymers and Their Potential for Nano-Patterning

Vishwanath Kalyani,[a] V. S. V. Satyanarayana,[a] Vikram Singh,[b] Chullikkattil P. Pradeep,*[a] Subrata Ghosh,[a] Satinder K. Sharma,[b] and Kenneth E. Gonsalves*[a]

Abstract: Two new polyoxometalate (POM)-based hybrid monomers $(Bu_4N)_5(H)[P_2V_3W_{15}O_{59}\{(OCH_2)_3CNHCO(CH_3)C{=}CH_2\}]$ (**2**) and $(S(CH_3)_2C_6H_4OCOC(CH_3){=}CH_2)_6[PV_2Mo_{10}O_{40}]$ (**5**) were developed by grafting polymerizable organic units covalently or electrostatically onto Wells–Dawson and Keggin-type clusters and were characterized by analytical and spectroscopic techniques including ESI-MS and/or single-crystal X-ray diffraction analyses. Radical initiated polymerization of **2** and **5** with organic monomers (methacryloyloxy)phenyldimethylsulfonium triflate (MAPDST) and/or methylmethacrylate (MMA) yielded a new series of POM/polymer hybrids that were characterized by ^1H, ^{31}P NMR and IR spectroscopic techniques, gel-permeation chromatography as well as thermal analyses. Preliminary tests were conducted on these POM/polymer hybrids to evaluate their properties as photoresists using electron beam (E-beam)/extreme ultraviolet (EUV) lithographic techniques. It was observed that the POM/polymer hybrid of **2** with MAPDST exhibited improved sensitivity under EUV lithographic conditions in comparison to the MAPDST homopolymer resist possibly due to the efficient photon harvesting by the POM clusters from the EUV source.

Introduction

Polyoxometalates (POMs) are a class of inorganic materials consisting of discrete, soluble, anionic metal oxide clusters of early transition metals like W, Mo, V, and Nb, exhibiting enormous versatility in their structural features and properties.[1] The properties as well as the processability of POM clusters can be enhanced by combining them with organic moieties, either electrostatically or covalently, resulting in organically modified POMs, which have found extensive applications in diverse fields.[2] One important class of functional materials containing POMs is POM/polymer hybrids. Polymers are among the most widely used materials and the incorporation of POM clusters into polymers is believed to improve their functionality and hence widen their scope of applications.[3] Judeinstein reported the first POM/polymer hybrid in 1992[4] and this concept was later developed by various other groups.[5–11] Today, the design and development of functional POM/polymer hybrids is an active research field targeting potential applications in areas like catalysis, electronics, biology, medicines, materials chemistry, electrochemistry, photocatalysis, and so on.[12]

Our research work focuses on the development of nonchemically amplified photoresist materials (n-CARs) for electron beam (E-beam) and extreme ultraviolet (EUV) lithography applications. In this regard, we have successfully developed a new organic monomer (4-(methacryloyloxy)phenyl)dimethylsulfonium triflate (MAPDST), which contains a polymerizable group at one end and an E-beam/EUV sensitive sulfonium moiety at the other.[13] Copolymers of MAPDST monomer are found to act as good photoresists for patterning up to 20 nm features under E-beam and EUV lithographic conditions.[13] In an effort to improve the sensitivity and thermal stability of organic n-CAR resist materials, we have envisaged the incorporation of POM clusters as inorganic components into such photoresist materials. This is because POMs contain metals of high atomic numbers and hence their absorption cross sections for X-rays and high-energy E-beam radiations are typically much higher than that for organic materials. In addition, the structural robustness of the POM clusters can impart thermal stability to the resist materials during prebake and postbake experimental conditions. Inorganic components tested earlier for improving resist properties include polyhedral oligomeric silsesquioxane (POSS)[14] and Hf nanoparticles.[15]

Herein, we report the synthesis and characterization of two new $[P_2V_3W_{15}O_{62}]^{9-}$ and $[PV_2Mo_{10}O_{40}]^{5-}$ cluster anions based hybrid monomers and their radical copolymerization with lithographically relevant organic monomers MAPDST and MMA to produce new POM/polymer hybrids. These new POM containing polymer hybrids were characterized and tested for their properties as n-CAR resist materials using E-beam and

[a] Dr. V. Kalyani, Dr. V. S. V. Satyanarayana, Dr. C. P. Pradeep, Dr. S. Ghosh, Prof. K. E. Gonsalves
School of Basic Sciences, Indian Institute of Technology Mandi
Mandi 175 001, Himachal Pradesh (India)
E-mail: pradeep@iitmandi.ac.in
kenneth@iitmandi.ac.in

[b] Dr. V. Singh, Dr. S. K. Sharma
School of Computing and Electrical Engineering
Indian Institute of Technology Mandi
Mandi 175001, Himachal Pradesh (India)

Supporting information for this article is available on the WWW under http://dx.doi.org/10.1002/chem.201405369.

EUV lithography studies. This study revealed that the incorporation of POMs into photoresist materials can lead to considerable increase in their EUV sensitivity.

Results and Discussion

The choice of the organic and POM precursors plays crucial role in determining the properties of the POM/polymer hybrids. In the present study, we selected MAPDST and MMA as organic monomers because of their known lithographic applications.[13] A vast majority of the reported POM/polymer hybrids contain smaller POM cluster types such as Lindqvist,[5] normal Keggin,[6] or Anderson[7]-type clusters or their derivatives. Herein, we used the mixed metallic Wells–Dawson-type cluster $(Bu_4N)_5(H)_4[P_2V_3W_{15}O_{62}]$[16] and Keggin-type cluster $H_5[PV_2Mo_{10}O_{40}]$[17,18] as POM precursors. These mixed metallic clusters are reported to exhibit good redox and catalytic properties.[17,8e]

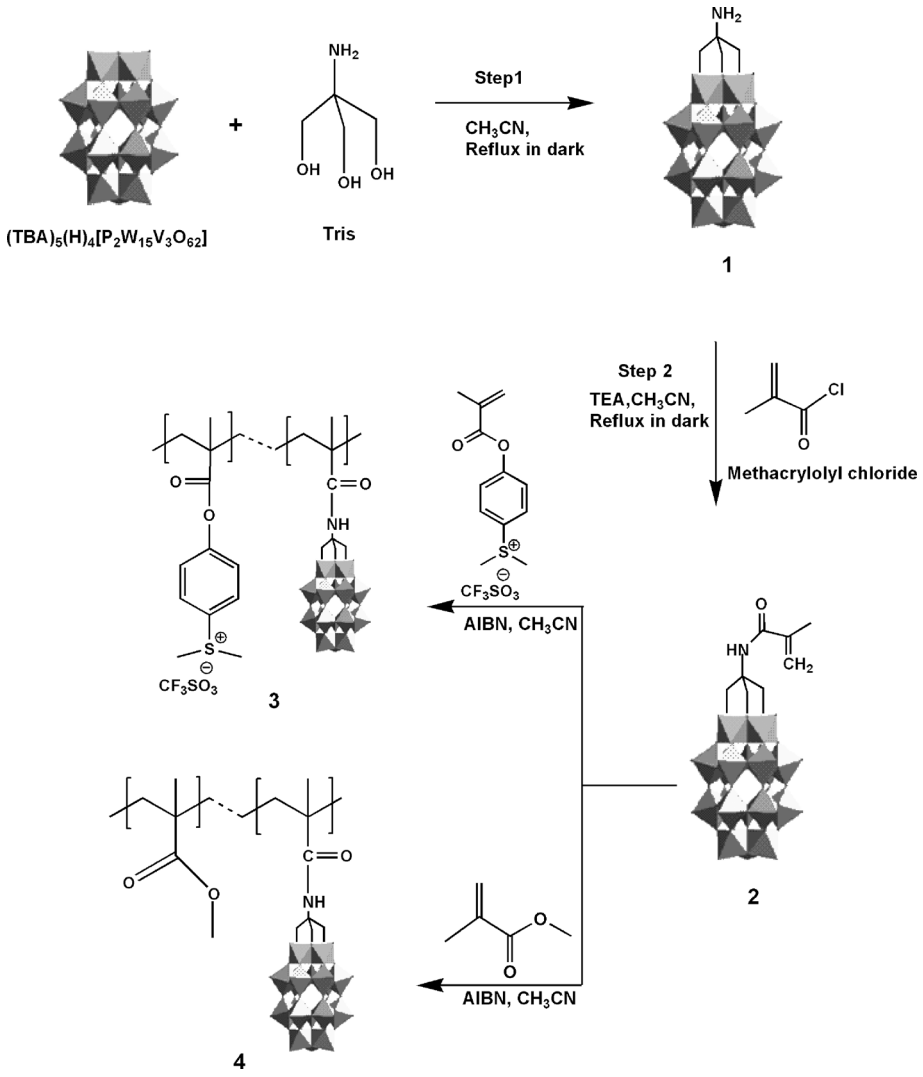

Scheme 1. Synthesis of Wells–Dawson-type hybrid monomer **2** and its polymerization with MAPDST and MMA monomers.

Various strategies are known for fabricating POM/polymer hybrids. These include physical blending of POMs and polymers,[9] in-situ polymerization in presence of POMs,[10] anchoring of POMs onto polymers through electrostatic interactions[11] and covalent binding of POMs onto polymer matrices.[5–8] All of these procedures are found to have some inherent limitations, but for the construction of stable POM/polymer hybrids, the electrostatic and covalent binding methods are found to be particularly useful.[3]

Synthesis and characterization of hybrid monomers

The synthetic scheme of $[P_2V_3W_{15}O_{62}]^{9-}$ cluster-based hybrid monomer $(Bu_4N)_5(H)[P_2V_3W_{15}O_{59}\{(OCH_2)_3CNHCO(CH_3)C{=}CH_2\}]$ (**2**), and its polymer hybrids with MAPDST and MMA monomers is given in Scheme 1. In the first step, tris(hydroxymethyl)aminomethane (Tris) was grafted onto the Wells–Dawson-type cluster $(Bu_4N)_5(H)_4[P_2V_3W_{15}O_{62}]$, in which three bridging oxygen atoms on the vanadium cap of the cluster get replaced with three hydroxyl oxygen atoms of the Tris moiety yielding the hybrid cluster **1**.[19] The hybrid monomer $(Bu_4N)_5(H)[P_2V_3W_{15}O_{59}\{(OCH_2)_3CNHCO(CH_3)C{=}CH_2\}]$ (**2**), was synthesized in 44% yield by treating the hybrid cluster **1** with methacryloyl chloride and triethylamine in acetonitrile under reflux conditions in the dark for 3 days.

The formation of the hybrid monomer **2** was confirmed by using ^{1}H NMR spectroscopy. A typical ^{1}H NMR spectrum of the hybrid monomer **2** is shown in Figure S1A in the Supporting Information. The peak observed at $\delta = 5.58$ ppm can be assigned to the methylene protons of the Tris moiety, which is a characteristic peak of the Tris-grafted Wells–Dawson-type $[P_2V_3W_{15}O_{62}]^{9-}$ clusters.[19] The methylene protons of the methacrylate group attached to the cluster appear at $\delta = 6.53$ and 5.63 ppm. The resonance signals of tetrabutylammonium (TBA) counterions appear between $\delta = 0.90$ and 3.16 ppm.

Further, formation of the hybrid monomer **2** was confirmed by ESI-MS analysis. Figure 1 shows the ESI-MS spectrum of hybrid monomer **2**. All the major peaks appearing in the mass spectrum could be satisfactorily assigned to the formula $[P_2V_3W_{15}O_{59}\{(OCH_2)_3CNHCO(CH_3)C{=}CH_2\}]^{6-}$ with various combinations of TBA and H counterions. For example, the

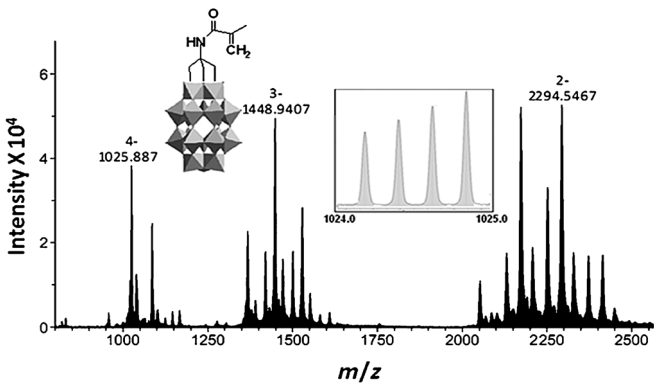

Figure 1. The molecular diagram and the negative-ion mode mass spectrum of the cluster anion **2**, $[P_2V_3W_{15}O_{59}\{(OCH_2)_3CNHCO(CH_3)C{=}CH_2\}]^{6-}$, taken in acetonitrile solution. The inset shows an expansion of the peak centered at 1025.88 to show its 4^- charge state.

peaks observed at *m/z* values 1025.88, 1448.94, and 2294.54 correspond to $H_2[P_2V_3W_{15}O_{59}\{(OCH_2)_3CNHCO(CH_3)C{=}CH_2\}]^{4-}$ $(Bu_4N)_1H_2[P_2V_3W_{15}O_{59}\{(OCH_2)_3CNHCO(CH_3)C{=}CH_2\}]^{3-}$, and $(Bu_4N)_2H_2[P_2V_3W_{15}O_{59}\{(OCH_2)_3CNHCO(CH_3)C{=}CH_2\}]^{2-}$, respectively (see the Supporting Information, Figure S3 a–d and Table S1 for assignment of all the peaks in the spectrum). The ESI-MS analysis therefore confirmed the formation of the hybrid monomer **2**.

It can be noted that majority of the reported POM-hybrid monomers contain more than one polymerizable organic moieties attached to the cluster. These include Keggin,[4,6] Lindqvist[5b,d], and Wells–Dawson-type[8a,d] cluster-based hybrid monomers. Hybrid monomers containing more than one polymerizable organic unit may lead to cross-linking and hence may adversely affect the possibility of forming linear polymers. The hybrid monomer **2** belongs to the small group of organic-POM hybrid monomers[5a,c,e, 8b,c,e–g] containing the POM and a polymerizable organic moiety attached in a 1:1 ratio.

The electrostatic binding of the cation of (methacryloyloxy)phenyl)dimethylsulfonium triflate (MAPDST) with Keggin-type polyoxomolybdate $H_5[PV_2Mo_{10}O_{40}].27H_2O$[17,18] was achieved by a counterion exchange process as depicted in Scheme 2. Here an aqueous solution of $H_5[PV_2Mo_{10}O_{40}]\cdot 27H_2O$ cluster was mixed with excess of MAPDST monomer in dichloromethane (CH_2Cl_2) solution. The counterion-exchanged Keggin-type cluster $(S(CH_3)_2C_6H_4OCOC(CH_3){=}CH_2)_6[PV_2Mo_{10}O_{40}]$, **5**, precipitated out as an orange powder during this process, was collected and washed with water and CH_2Cl_2. The hybrid monomer **5** is insoluble in water as well as in CH_2Cl_2 but is readily soluble in dimethylformamide (DMF) and dimethylsulfoxide (DMSO) solvents at room temperature. The hybrid monomer **5** was characterized by ^1H NMR and IR spectroscopic techniques. The ^1H NMR spectrum of **5** showed characteristic resonance signals at $\delta = 7.57$–8.17, 5.96–6.31, and 3.26 ppm (Figure S1B in the Supporting Information), which can be assigned to the aromatic, vinyl ($C{=}CH_2$) and $S(CH_3)_2$ protons of the (methacryloyloxy)-phenyldimethylsulfonium counterions, respectively. The formation of the Keggin-type cluster based hybrid monomer **5** was further confirmed by IR spectroscopy. The IR spectrum of the hybrid monomer **5** (Figure S4e, 2, in the Supporting Information) shows the expected bands of Mo=O and Mo–O–Mo stretching vibrations at 942 and 869, 785 cm^{-1} respectively. The presence of (methacryloyloxy)phenyldimethylsulfonium counterion is confirmed by the presence of a peak at 1733 cm^{-1} due to C=O stretching vibrations. The peaks observed at 2928 and 3018 cm^{-1} are assigned to C–H stretching vibrations of methyl group.

It is observed that during the counterion-exchange process, reduction of the Keggin-type cluster anion, $[PV_2Mo_{10}O_{40}]^{5-}$ occurs, which increases its charge from 5^- to 6^-. Six (methacryloyloxy)phenyldimethylsulfonium cations from the MAPDST monomers replace all of the H^+ counterions of the Keggin-type cluster effectively. This observation was confirmed by single-crystal X-ray analysis. Single crystals of this compound were grown from DMSO solutions by ether diffusion.

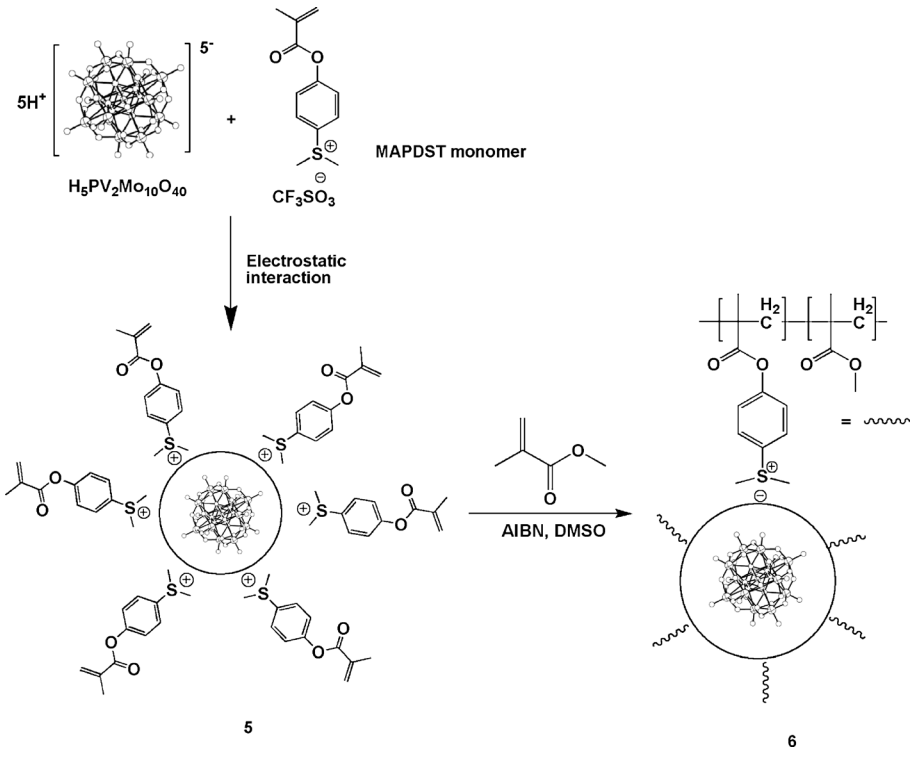

Scheme 2. Synthetic pathway for the preparation of hybrid monomer **5** and its POM/polymer hybrid **6** with MMA.

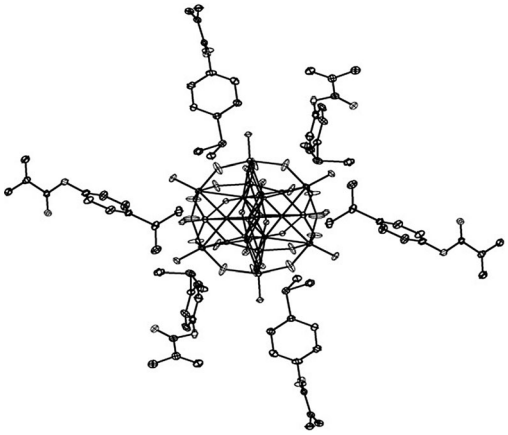

Figure 2. ORTEP representation of the (methacryloyloxy)phenyldimethylsulfonium)$_6$[$PV_2Mo_{10}O_{40}$] cluster **5**.

Single-crystal X-ray analysis revealed that the structure of the hybrid monomer **5** consists of six (methacryloyloxy)phenyldimethylsulfonium counterions arranged symmetrically around the $[PV_2Mo_{10}O_{40}]^{6-}$ cluster anion as shown in Figure 2. Crystallographic data for the hybrid monomer **5** are compiled in Table S2 of the Supporting Information.

The counterion-exchanged Keggin-type hybrid monomer **5** is an interesting compound for more than one reason. Firstly, it contains a sulfonium-based functional cation that acts as efficient counterion, replacing even H^+ counterions of the cluster. Secondly, the hybrid monomer **5** belongs to the rare class of POM clusters having sulfonium counterions. To the best of our knowledge, only a few such compounds are reported earlier in the literature.[20] Sulfonium counterion POMs are useful as photochromic materials.[20a] Moreover, such clusters having multiple polymerizable moieties disposed symmetrically around the cluster moiety could be useful as precursors for the synthesis of hybrid supramolecular star polymers.[21]

POM/polymer hybrid synthesis and characterization

The Wells–Dawson-type cluster-based hybrid monomer **2** and Keggin-type cluster-based hybrid monomer **5** were subjected to free-radical polymerization reactions with the organic monomers MAPDST[13] and MMA using one weight% of 2,2′-azobis(2-methylpropionitrile (AIBN) as the radical initiator in acetonitrile and DMSO solutions, respectively, under N_2 atmosphere (as shown in Schemes 1 and 2). The complete inertness of the reaction medium was ensured by applying several freeze–thaw cycles. After drying, the reaction vessel was kept in a constant temperature oil bath at 70 °C for two days.

The radical polymerization reaction between the hybrid monomer **2** and organic MAPDST monomer yielded a viscous product, which was added drop-wise into an excess of diethyl ether solution resulting in a brownish yellow solid of the POM/polymer hybrid **3** in 67% yield. Similarly, the viscous reaction products obtained from the polymerization reactions between the hybrid monomers **2** and **5** with MMA monomer were added drop-wise into excess of methanol to precipitate the corresponding yellow-colored solid products of POM/polymer hybrids **4** and **6** in 45 and 64% yields, respectively.

The POM/polymer hybrids thus obtained were characterized by using various analytical techniques such as IR, NMR spectroscopies, gel-permeation chromatography (GPC) and TGA/DSC analyses. Figure 3 shows the ^{1}H NMR spectra of the POM/polymer hybrids **3**, **4**, and **6** in [D_6]DMSO and $CDCl_3$ solvents. The spectrum of **3** (Figure 3A) shows broad peak in the range of $\delta = 1.0$ to 1.7 ppm, which can be assigned to the methyl protons, whereas the broad peak observed in the range of $\delta =$ 1.8 to 2.8 ppm corresponds to the polymeric methylene protons from the MAPDST chain.[13] The resonance signal appearing at $\delta = 3.21$ ppm can be ascribed to the methyl protons attached to the sulfonium group of the MAPDST moiety. The signals due to the aromatic protons of the MAPDST moiety appear between $\delta = 7.41$–8.01 ppm. In the present case, we assume that the ^{1}H NMR signals due to the hybrid cluster **2** and its counterions are absent because of very low percentage of POM clusters in the polymer. Similar cases have been reported earlier.[7c,8b] However, the incorporation of POM clusters in the polymer is confirmed by ^{31}P NMR studies. The ^{31}P NMR spectrum of hybrid **3** (Supporting Information, Figure S2A) shows two phosphorous resonances at $\delta = -6.812$ and -13.008 ppm corresponding to the phosphate groups connected to the V_3 and W_3 caps of the cluster, respectively. The presence of POM clusters in the hybrid **3** is also confirmed by EDX analyses (Figure S6A in Supporting Information). ^{19}F NMR analysis (Figure S1C in the Supporting Information) of **3** shows a peak at $\delta = -77.6$ ppm, corresponding to the $CF_3SO_3^-$ anionic part of the MAPDST moiety. Based on these observation, a plausible structure for the POM/polymer hybrid **3** is proposed as shown in Scheme 1.

The ^{1}H NMR spectrum of POM/polymer hybrid **4** is shown in Figure 3B. Here, the disappearance of the olefinic proton peaks of MMA as well as the hybrid monomer **2** confirms the completeness of the polymerization. The broad peak appearing between $\delta = 1.14$–2.0 ppm corresponds to the methylene protons of the polymeric chain. The dominating methyl proton signals from both MMA and POM hybrid moieties appear at $\delta = 0.76$–0.95 ppm. The characteristic signal of $-OCH_3$ protons from MMA moiety appears at $\delta = 3.53$ ppm. The absence of peaks corresponding to the hybrid POM unit in the ^{1}H NMR spectrum of **4** could be due to the limited number of POM clusters in the polymer.[7c,8b] However, the ^{31}P NMR spectrum of **4** (Supporting Information, Figure S2B) shows two phosphorous resonances at $\delta = -6.716$ and -12.957 ppm corresponding to the phosphate groups connected to the V_3 and W_3 caps of the cluster respectively, confirming the incorporation of POM cluster in the polymer. EDX studies (Figure S6B in the Supporting Information) also confirmed the presence of POM cluster in **4**.

The ^{1}H NMR spectrum of the hybrid **6** is presented in Figure 3C. The resonance of methyl protons from MMA and MAPDST units appear between $\delta = 0.84$ and 1.0 ppm. The broad peaks observed between $\delta = 1.21$ to 2.0 ppm can be assigned to the polymeric methylene protons. The signal at $\delta =$ 3.60 ppm can be assigned to the methyl protons attached to

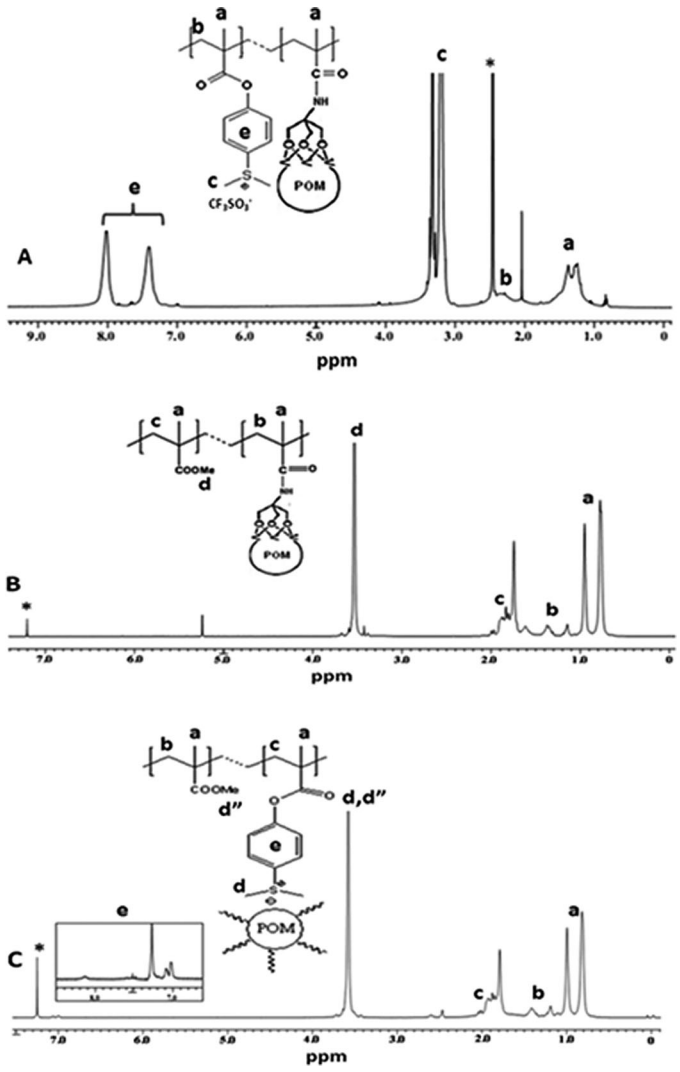

Figure 3. ^{1}H NMR spectra of POM/polymer hybrids: A) **3** (* the peak of $[D_6]$DMSO); B) **4**, and C) **6** (* the peak of $CDCl_3$).

the sulfonium group of MAPDST unit as well as methoxy group of MMA together. The aromatic protons of phenyl ring are observed between $\delta = 7.05$–8.13 ppm. The ^{19}F NMR spectrum (Figure S1D in the Supporting Information) of the hybrid **6** showed the absence of $CF_3SO_3^-$ unit, confirming the complete counterion exchange of the $[PV_2Mo_{10}O_{40}]^{5-}$ cluster with (methacryloyloxy)phenyldimethylsulfonium counterions as observed earlier. Further, ^{31}P NMR analysis of hybrid **6** (Supporting Information, Figure S2C) showed a phosphorous signal at $\delta = -3.852$ ppm, confirming the incorporation of hybrid monomer **5** in the polymer. ICP-AES analysis showed the presence of 3.7% of Mo and 0.4% V in the sample, further confirming the inclusion of the POM cluster in the polymer.

IR spectroscopy is a common tool to prove the presence of various functional groups in a compound. As shown in Figure S4a in the Supporting Information, the IR spectrum of the Wells–Dawson-type cluster-based hybrid monomer **2** shows peaks due to tetrabutylammonium counterions in the region 2800 to 3000 cm^{-1} and characteristic POM anion bands between 600 to 1200 cm^{-1}. The IR spectrum of hybrid **3** (Figure S4b in the Supporting Information) shows bands at 3028 and 2932 cm^{-1} due to C–H stretching vibrations of the methyl group. An intense band observed at 1755 cm^{-1} can be assigned to the C=O stretching vibrations, confirming the presence of MAPDST unit in this hybrid. The presence of POM cluster in hybrid **3** is indicated by the presence of characteristic peaks at 1170, 1099, and 1028 cm^{-1} due to P–O and at 810 and 630 cm^{-1} due to W–O–W vibrations.

The IR spectrum of POM/polymer hybrid **4** (Figure S4c in the Supporting Information), exhibited absorption bands at 1731 and 1271 cm^{-1}, corresponding to the C=O and $-OCH_3$ stretching vibrations of its MMA units. The anionic part of the Wells–Dawson-type cluster showed characteristic absorption bands in the region of 600 to 1200 cm^{-1}, in which the bands at 1195 and 1059 are assigned to the P–O vibrations and bands at 988, 964, 835, and 753 cm^{-1} are assigned to the V=O, W=O, W–O–W stretching vibrations, respectively.

The IR spectrum of POM/polymer hybrid **6** is given in Figure S4d (in the Supporting Information), which shows the characteristic Mo=O, V=O vibrations due to $[PV_2Mo_{10}O_{40}]$ cluster appearing at 964 and 985 cm^{-1} and P–O stretching peaks at 1193, 1147, and 1058 cm^{-1}, respectively. The IR spectrum of **6** also shows bands at 2998, 2945, and 2856 cm^{-1}, assigned to the C–H stretching vibrations of methyl group, whereas the band appearing at 1731 cm^{-1} is ascribed to the C=O stretching vibrations of MMA units.

Molecular weight determination and thermal properties

The POM/polymer hybrids **3**, **4**, and **6** are soluble in organic solvents such as acetonitrile, DMF, chloroform, and CH_2Cl_2 at room temperature, which enabled their molecular weight determination by using gel-permeation chromatography (GPC). The GPC analyses of the hybrids **3**, **4**, and **6** were performed at 25 °C using DMF or chloroform as mobile phase. The relative molecular weights were determined by using different polystyrene standards. The molecular weights, polydispersity index, and thermal properties of these hybrids are summarized in Table 1.

Table 1. Summary of the characterization data for POM/polymer hybrids.

POM/polymer/hybrid	Yield [%]	T_d[a] [°C]	M_w [g mol^{-1}]	PDI[b]
3	67	250	14000	1.5
4	45	247	30000	1.8
6	64	270	44000	2.2

[a] Decomposition temperature (5% weight loss). [b] Polydispersity index.

The weight average molecular weight (M_w) of the hybrid **3** is found to be 14.0×10^3 with a polydispersity index of 1.5 whereas, the M_w of the hybrid **4** is found to be 30×10^3 with a polydispersity index of 1.87. The M_w of **6** is 44.0×10^3 with a polydispersity index of 2.21. Some of the previously reported POM–MMA hybrids also exhibited comparable molecular weights.[8a]

Thermogravimetric analysis (TGA) and differential scanning calorimetry (DSC) were carried out on samples of POM/polymer hybrids **3**, **4**, and **6** under a nitrogen atmosphere. TGA profiles of the hybrids are shown in Figure S5 (see the Supporting Information). These studies showed that the hybrids **3**, **4**, and **6** are thermally stable up to approximately 245 °C and above this temperature, they start to decompose. A continuous and major weight loss was observed in the range of 245 to 450 °C for all the hybrids, most probably due to the polymer and cluster disintegration. The decomposition temperatures of hybrids **3** and **4** were found to be 250 and 247 °C, respectively (T_d, 5% weight loss). The hybrids **3** and **4** showed residual masses at 800 °C of 9.49 and 7.34%, respectively, most probably due to their metal oxide residues. In the case of hybrid **6**, the decomposition temperature was found to be 270 °C (T_d, 5% weight loss). The DSC profiles of the POM/polymer hybrids are given in Figure S5 (see the Supporting Information). The DSC profile of hybrid **3** showed one endothermic peak at 133.3 °C corresponding to its glass transition temperature (T_g). The glass transition temperature of hybrid **4** is found to be 132.5 °C whereas, the hybrid **6** exhibits a glass transition temperature of 131.8 °C. All of these POM/polymer hybrids showed enhanced decomposition temperature (T_d) in comparison to the corresponding organic polymers,[13c] probably due to the cluster attachment.

The residual mass of 9.49 and 7.34% due to metal oxides observed in the TGA profiles of POM/polymer hybrids **3** and **4**, respectively, suggest the presence of about 0.3 and approximately 0.5 POM cluster per polymer chain considering their molecular weights given in Table 1. Similarly, the residual mass of 6.30% observed in the case of hybrid **6** suggests the presence of approximately 1.7 cluster per polymer chain. The low percentages of POM clusters in these polymers are consistent with their NMR data in which the peaks due to the organic monomers were dominating, making it difficult to observe the peaks due to hybrid clusters and their counterions.

Lithography studies

Preliminary tests on the POM/polymer hybrids **3**, **4**, and **6** towards their non-chemically amplified resist (n-CARs) application were conducted by using E-beam lithography studies. Solutions (2 wt%) of the POM/polymer hybrids were prepared in acetonitrile/anisole solvents and were spin-coated on hexamethyldisilazane (HMDS)-treated RCA-cleaned p-type Si wafer pieces (2×2 cm in size) to obtain films of approximately 35 nm thickness. These films were then exposed at Raith-150 E-beam lithography (EBL) system using 20 keV energy for doses 30, 35, 40, 45, 50, and 75 $\mu C\,cm^{-2}$ with an aperture size of 20 μm. EBL exposure studies (see the Supporting Information for the Experimental Details) on the POM/polymer hybrid **3** resist showed good line patterns up to 22 nm size as depicted in Figure S7 (see the Supporting Information), indicating its potential as photoresist material. Thin films of the hybrid polymers **4** and **6** did not show good line patterns under similar experimental conditions, probably because of their composition differences compared to hybrid **3**.

Encouraged from the preliminary EBL exposure results, resists prepared from POM/polymer hybrid **3** were subjected to EUV exposure studies using SEMATECH Berkeley Microfield Exposure Tool (MET), which is a high-resolution EUV (13.5 nm) lithography tool. The resist solution was spin-coated on HMDS treated silicon wafer and prebaked at 100 °C for 90 s to give a film of thickness approximately 35 nm. Firstly, test wafers were run to calculate the E_o center dose value for the hybrid **3** resist. An E_o center dose value of 8.5 $mJ\,cm^{-2}$ was obtained, which is roughly 3 times lower than that obtained for the pure MAPDST homopolymer resist (30 $mJ\,cm^{-2}$).[13c] This indicates that the sensitivity of the POM/polymer hybrid **3** increased roughly three times compared with the pure organic homopolymer resist probably due to the efficient EUV photon harvesting by the POM clusters, which is a desirable outcome of this study. For high-resolution line patterns, the resist sample was exposed using mask IMO228775 with Field of R4C3 and post-exposure bake was given at 115 °C for 90 s. After the EUV exposure, the sample was developed with TMAH-based developer for 8 s, rinsed in DI water for 10 s and blow-dried using nitrogen gas. The photon-directed polarity change occurs at the sulfonium centers of the polymer resist causing solubility differences to the exposed and un-exposed regions during development leading to pattern formation.[13] A high-resolution circular EUV pattern obtained for POM/polymer hybrid **3** resist is shown in Figure 4 (see the Supporting Information, Figure S9 a–c for additional EUV figures). Further EUV optimization studies are currently underway to obtain sub 20 nm line patterns for hybrid **3**. The present study therefore reveals that the incorporation of Wells–Dawson-type cluster $[P_2V_3W_{15}O_{62}]^{9-}$ into the organic photoresist material enhances the sensitivity of the photoresist considerably under EUVL conditions.

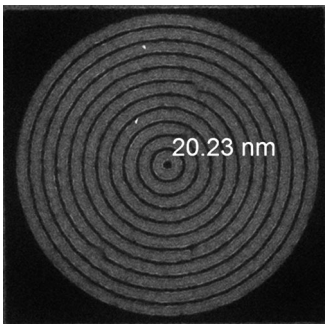

Figure 4. EUV patterned 20 nm circular images with 70 nm space for POM/polymer hybrid **3** resist using MET at SEMATECH Berkeley.

Conclusion

We have successfully synthesized two new organic-POM hybrid monomers starting from Wells–Dawson and Keggin-type clusters and subjected them to radical polymerization with lithographically relevant organic monomers to yield new POM/polymer hybrids. These new POM/polymer hybrids show improved decomposition and glass transition temperatures in comparison to their pure organic polymer counterparts. Further, pre-

liminary studies on these hybrids towards their non-chemically amplified resist application were conducted using E-beam and EUV lithography techniques. It was observed that the hybrid **3**, based on $[P_2V_3W_{15}O_{59}\{(OCH_2)_3CNHCO(CH_3)C{=}CH_2\}]^{6-}$ and MAPDST monomer, is capable of patterning up to 20 nm line features under E-beam as well as EUV exposure conditions. It was found that the inclusion of POM clusters in hybrid **3** resulted in enhanced sensitivity in comparison to the MAPDST homopolymer resist. The present approach may pave the way for improved hybrid n-CARs thus resulting in efficient materials for semiconductor industries. More optimization studies on these hybrids towards their lithographic applications are currently underway.

Experimental Section

Materials

Triethylamine and acetonitrile were distilled over CaH_2 and acetonitrile was further dried over 4 Å molecular sieves prior to the use. The MAPDST monomer and methacryloyl chloride were synthesized according to the literature procedures.[13] Methyl methacrylate (MMA) was freshly distilled prior to the use. The Wells–Dawson-type $(Bu_4N)_5(H)_4[P_2V_3W_{15}O_{62}]$[16] polyoxometalate and Keggin-type $H_5[PV_2Mo_{10}O_{40}]\cdot 27\,H_2O$[17,18] polyoxomolybdate were prepared according to the reported literature procedures. DMSO and CH_2Cl_2 were purchased from Sigma–Aldrich and were used as received. Tetramethylammoniumhydroxide (TMAH), methyl isobutyl ketone (MIBK), and isopropyl alcohol (IPA) were purchased from Microchem and were used as received.

Characterization

The ^1H and ^{31}P NMR spectra were recorded on 500 and 400 MHz JEOL NMR spectrometers, respectively, in $[D_6]$DMSO and $CDCl_3$ solvents. FTIR spectra were recorded using KBr pellets on PerkinElmer Spectrum 2 instrument. Thermogravimetric analyses (TGA) were performed on a Netzsch Model STA 449 F1 JUPITER instrument at a heating rate of 10 °C min^{-1} under N_2 atmosphere. ESI-MS analyses were conducted on a Bruker Mass spectrometer instrument at 180 °C in acetonitrile solvent and data were recorded in negative-ion mode. GPC measurements were recorded on a Thermo Quest GPC at 25 °C using DMF and $CHCl_3$ as mobile phase. The analyses were carried out at a flow rate of 1 mL min^{-1} using Styragel HT column packed with rigid 10 μm particles. The columns were calibrated with different polystyrene standards. The ICP-AES analyses were conducted on ARCOS instrument from M/s Spectro, Germany, Radical plasma, Wavelength Range: 130 to 770 nm with Charge Coupled Devices (CCD) detector. The samples for ICP analyses were prepared by dissolving the polymer in aqua-regia followed by heating. $HClO_4$ was added to the boiling solution drop-wise and heating continued until the entire polymer is destroyed. The solution was then diluted with distilled water.

X-ray crystallographic analysis

Single-crystal X-ray data were collected at 293(2) K on a Bruker SMART APEX CCD diffractometer using graphite-monochromated $Mo_{K\alpha}$ radiation ($\lambda = 0.71073$ Å). The data were reduced using SAINTPLUS[22] and a multi-scan absorption correction using SADABS[22] was performed. The structure was solved by direct methods and refined on F^2 by full-matrix least-squares procedure using the SHELX-97 program.[23] Non-hydrogen atoms were refined anisotropically. Hydrogen atoms were introduced on calculated positions and included in the refinement riding on their respective parent atoms. CCDC-1007244 contains the supplementary crystallographic data for this paper. These data can be obtained free of charge from The Cambridge Crystallographic Data Centre via www.ccdc.cam.ac.uk/data_request/cif.

Syntheses

Hybrid monomer 2

Methacryloyl chloride (0.018 g, 0.17 mmol) was added to a solution of compound **1**[19c] (0.9 g, 0.17 mmol) and triethylamine (TEA) (0.069 g, 0.68 mmol) in dry acetonitrile (10 mL) and the resulting mixture was heated at reflux in the dark for 3 days. The dark-brown colored reaction mixture thus obtained was cooled down to room temperature and filtered to remove any white solid (triethylamine salt). The dark filtrate was then added dropwise into excess of diethyl ether to precipitate out a fine yellow colored powder, which was collected by filtration, washed with ether, and dried under vacuum to afford hybrid monomer **2**. Yield: 400 mg (44%); ^1H NMR (500 MHz, $[D_6]$DMSO, 25 °C): $\delta = 7.38$ (1H, s, NH), 6.53 (1H, s, C=CH), 5.63 (1H, s, C=CH), 5.58 ppm (6H, s, CH_2O) in addition to counterion resonances; IR (KBr): $\tilde{\nu} = 2962$, 2938, 2871 (C–H), 1696 (CONH), 1117, 1066, 1030 (P–O), 940 (V=O), 921 (W=O), 666 cm^{-1} (M–O–M) vibrations; MS (70 eV): *m/z*: calcd: 1026.88 $[H_2P_2V_3W_{15}O_{59}C_8H_{12}NO_4]^{4-}$; observed: 1025.88.

Hybrid monomer 5

In a typical preparation, Keggin-type POM $[H_5PV_2Mo_{10}O_{40}]\cdot 27\,H_2O$ (1.0 g, 0.44 mmol) was dissolved in deionized water (5 mL) and stirred for five minutes to obtain a clear red-orange solution. At the same time, 1.05 g (2.81 mmol) of MAPDST (4-(methacryloyloxy)-phenyl)dimethylsulfoniumtriflate) monomer was dissolved in dichloromethane (5 mL) and stirred for five minutes. The obtained clear solution of MAPDST monomer was slowly added to an aqueous solution of POM under constant stirring for 30 min in the dark. The orange-colored solid of hybrid monomer **5** thus obtained was washed thoroughly with water and dichloromethane to remove any unreacted starting materials and finally dried in an oven at 40 °C for 24 h. Yield: 900 mg (51%); ^1H NMR (500 MHz, $[D_6]$DMSO, 25 °C): $\delta = 8.16$ (2H, d, $J = 8.75$ Hz, *m,m′*-ArH), 7.58 (2H, d, $J = 8.75$ Hz, *o,o′*-ArH), 6.31 (1H, s, C=CH), 5.96 (1H, s, C=CH), 3.26 (6H, s, $S(CH_3)_2$), 2.0 ppm (3H, s, CH_3); IR (KBr): $\tilde{\nu} = 3018$, 2928 (C–H), 1733 (C=O), 1632, 1581, 1492 (ArC=C), 1172, 1116, 1048 (P–O), 942 (Mo=O) 869, 785 cm^{-1} (Mo–O–Mo) stretching vibrations. Red-orange colored tiny single crystals of hybrid monomer **5** were grown by slow diffusion of diethyl ether into DMSO solution.

Polymerization

All polymerization reactions were carried out under nitrogen atmosphere using freeze-pump-thaw technique for degassing the reaction mixture.

POM/polymer hybrid 3

Wells–Dawson type hybrid monomer **2** (0.1 g, 0.018 mmol), MAPDST monomer (0.9 g, 2.41 mmol), 2,2′-azobis(2-methylpropionitrile (AIBN) (10 mg, 0.060 mmol), and dry CH_3CN (3 mL) were added to a dry Schlenk flask, under N_2 atmosphere. After several freeze-pump-thaw cycles, the flask was placed in a constant temperature oil bath kept at 70 °C for 2 days in dark. The polymeri-

zation was stopped by cooling the flask to the room temperature. The viscous reaction mixture thus obtained was then added dropwise into excess of diethyl ether to get a brownish-yellow colored solid. The obtained solid was washed three times with ether and dried in an oven at 40 °C overnight. Yield: 670 mg (67 %); ^{1}H NMR (400 MHz, [D$_6$]DMSO, 25 °C): δ = 8.01 (2 H, s br, *m,m′*-ArH), 7.41 (2 H, s br, *o,o′*-ArH), 3.21 (6 H, s, S(CH$_3$)$_2$), 1.8–2.8 (2 H, br peak, CH$_2$), 1.0–1.7 ppm (3 H, br peak, CH$_3$); ^{31}P NMR (400 MHz, [D$_6$]DMSO, 25 °C) δ = −6.812 (s, 1 P), −13.008 ppm (s, 1 P); ^{19}F NMR (500 MHz, [D$_6$]DMSO, 25 °C): δ = −77.6 ppm (3F, s, CF$_3$); IR (KBr): $\tilde{\nu}$ = 3028, 2932 (C–H), 1755 (C=O), 1260 (OCH$_3$), 1170, 1099, 1028 (P–O), 990 (V=O), 920 (W=O), 810, 630 cm^{-1} (M–O–M) vibrations; GPC (DMF, eluent): M_n = 9090, PDI = 1.5.

POM/polymer hybrid 4

Wells–Dawson-type hybrid monomer **2** (0.1 g, 0.018 mmol), MMA (0.9 g, 8.98 mmol), AIBN (10 mg, 0.060 mmol), and dry CH$_3$CN (3 mL) were added to a dry Schlenk flask, under N$_2$ atmosphere and left stirring at 70 °C for 2 days in dark. The viscous reaction mixture thus obtained was then added drop-wise into excess of methanol to get a brownish-yellow colored solid. Yield: 450 mg (45 %); ^{1}H NMR (500 MHz, CDCl$_3$, 25 °C): δ = 3.53 (3 H, s, OCH$_3$), 1.14–2.0 (2 H, br peak, CH$_2$), 0.76–0.95 ppm (3 H, 2 s, CH$_3$); ^{31}P NMR (400 MHz, CDCl$_3$, 25 °C) δ = −6.716 (s, 1P), −12.957 ppm (s, 1P); IR (KBr): $\tilde{\nu}$ = 2998, 2957, 2839 (C–H), 1731 (C=O), 1271, 1242 (OCH$_3$), 1195, 1148, 1059 (P–O), 988 (V=O), 964 (W=O) and 835, 753 cm^{-1} (M–O–M) stretching vibrations. GPC (CHCl$_3$, eluent): M_n = 16 000, PDI = 1.87.

POM/polymer hybrid 6

Hybrid monomer **5** (0.1 g, 0.032 mmol), MMA (0.9 g, 8.98 mmol), and AIBN (10 mg, 0.060 mmol) were added To a dry Schlenk flask, in dry DMSO solvent (3 mL) under N$_2$ atmosphere and left stirring at 70 °C for 2 days in dark. The viscous reaction mixture thus obtained was then added drop-wise into excess of methanol to get a brownish-yellow colored solid. Yield: 640 mg (64 %); ^{1}H NMR (500 MHz, CDCl$_3$, 25 °C): δ = 8.13 (2 H, s, *m,m′*-ArH), 7.05 (2 H, s, *o,o′*-ArH), 3.60 (6 H, s, S(CH$_3$)$_2$), 1.21–2.0 (2 H, br peak, CH$_2$), 0.84–1.0 ppm (3 H, 2 s, CH$_3$); ^{31}P NMR (400 MHz, CDCl$_3$, 25 °C) δ = −3.852 ppm (s, 1 P); IR (KBr): $\tilde{\nu}$ = 2998, 2945, 2856 (C–H), 1731 (C=O), 1272, 1241 (OCH$_3$), 1193, 1147, 1058 (P–O), 985 (V=O), 964 (Mo=O), 805, 750 cm^{-1} (Mo–O–Mo) vibrations. GPC (CHCl$_3$, eluent): M_n = 19 800, PDI = 2.21.

Resist preparation

2 wt % resist solutions of the POM/polymer hybrids **3**, **4**, and **6** were prepared in acetonitrile and anisole solvents, and were spin-coated on HMDS-treated RCA-cleaned p-type Si wafer pieces of 2 × 2 cm size to obtain approximately 35 nm thick films. The prebake annealing of the hybrid resist samples were performed at 115 °C for 90 s on a hot plate. After the prebake annealing, samples were exposed at Raith-150 E-beam system using 20 keV energy for different doses 30, 35, 40, 45, 50, and 75 μC cm^{-2} with an aperture size of 20 μm. Exposed POM/polymer hybrid **3** samples were developed in optimized TMAH-based DI developer (aqueous solutions of TMAH in DI water maintained at pH ≈ 11.5) at room temperature for 8 s, rinsed in de-ionized water for about 5 to 8 s and blow dried with pure nitrogen gas. In similar fashion, hybrids **4** and **6** were developed in standard 1:3 methylisobutylketone (MIBK) solution for 30 s followed by 15 s in isopropylalcohol (IPA).

Imaging

Developed resist samples were carefully examined with SEM attached to Raith 150 lithography system at energy of 5 keV. HR-SEM images were taken using Nova Nano SEM 450 FEI instrument.

Acknowledgements

We received partial support from Intel Corp USA. The use of Berkeley BMET tool for EUV exposures is also acknowledged. IIT Mandi acknowledges the use of the Center of Excellence in Nanoelectronics (CEN) facilities at IIT Bombay under the Indian Nanoelectronics Users Programme (INUP), India.

Keywords: cluster compounds · NMR spectroscopy · organic–inorganic hybrid composites · polymers · polyoxometalates

[1] a) M. T. Pope, A. Müller, *Introduction to Polyoxometalate Chemistry from Topology via Self-Assembly to Applications*, Kluwer, Dordrecht, **2001**, pp. 1–6; b) C. L. Hill, *Chem. Rev.* **1998**, *98*, 1–2; c) D.-L. Long, R. Tsunashima, L. Cronin, *Angew. Chem. Int. Ed.* **2010**, *49*, 1736–1758; *Angew. Chem.* **2010**, *122*, 1780–1803.

[2] a) A. Dolbecq, E. Dumas, C. R. Mayer, P. Mialane, *Chem. Rev.* **2010**, *110*, 6009–6048; b) S. Berardi, M. Carraro, A. Sartorel, G. Modugno, M. Bonchio, *Isr. J. Chem.* **2011**, *51*, 259–274; c) A. Proust, R. Thouvenot, P. Gouzerh, *Chem. Commun.* **2008**, 1837–1852; d) A. Dolbecq, P. Mialane, F. Sécheresse, B. Keita, L. Nadjo, *Chem. Commun.* **2012**, *48*, 8299–8316.

[3] W. Qi, L. Wu, *Polym. Int.* **2009**, *58*, 1217–1225.

[4] P. Judeinstein, *Chem. Mater.* **1992**, *4*, 4–7.

[5] a) A. R. Moore, H. Kwen, A. M. Beatty, E. A. Maatta, *Chem. Commun.* **2000**, 1793–1794; b) L. Xu, M. Lu, B. B. Xu, Y. G. Wei, Z. H. Peng, D. R. Powell, *Angew. Chem. Int. Ed.* **2002**, *41*, 4129–4132; *Angew. Chem.* **2002**, *114*, 4303–4306; c) B. Xu, M. Lu, J. Kang, G. Wang, J. Brown, Z. H. Peng, *Chem. Mater.* **2005**, *17*, 2841–2851; d) L. Meng, B. Xie, J. H. Kang, T. Chen, Y. Yang, Z. H. Peng, *Chem. Mater.* **2005**, *17*, 402–408; e) S. Chakraborty, A. Keightley, V. Dusevich, Y. Wang, Z. H. Peng, *Chem. Mater.* **2010**, *22*, 3995–4006.

[6] a) C. R. Mayer, V. Cabuil, T. Lalot, R. Thouvenot, *Angew. Chem. Int. Ed.* **1999**, *38*, 3672–3675; *Angew. Chem.* **1999**, *111*, 3878–3881; b) C. R. Mayer, I. Fournier, R. Thouvenot, *Chem. Eur. J.* **2000**, *6*, 105–110; c) H. G. Chen, L. Xie, H. B. Lu, Y. L. Yang, *J. Mater. Chem.* **2007**, *17*, 1258–1261; d) J. L. Horan, A. Genupur, H. Ren, B. J. Sikora, M. C. Kuo, G. M. Haugen, M. A. Yandrasits, S. J. Hamrock, M. H. Frey, A. M. Herring, *ChemSusChem* **2009**, *2*, 226–229; e) M. Carraro, G. Fiorani, L. Mognon, F. Caneva, M. Gardan, C. Maccato, M. Bonchio, *Chem. Eur. J.* **2012**, *18*, 13195–13202.

[7] a) D. Schaming, C. Allain, R. Farha, M. Goldmann, S. Lobstein, A. Giraudeau, B. Hasenknopf, L. Ruhlmann, *Langmuir* **2010**, *26*, 5101–5109; b) N. Xia, W. Yu, W. Wang, G. Sakaguchi, H. Hasegawa, *Polymer* **2011**, *52*, 1772–1780; c) B. Hu, C. Wang, J. Wang, J. Gao, K. Wang, J. Wu, G. Zhang, W. Cheng, B. Venkateswarlu, M. Wang, P. S. Lee, Q. Zhang, *Chem. Sci.* **2014**, *5*, 3404–3408.

[8] a) T. Hasegawa, H. Murakami, K. Shimizu, Y. Kasahara, S. Yoshida, T. Kurashina, H. Seki, K. Nomiya, *Inorg. Chim. Acta* **2008**, *361*, 1385–1394; b) Y. K. Han, Y. Xiao, Z. J. Zhang, B. Liu, P. Zheng, S. J. He, W. Wang, *Macromolecules* **2009**, *42*, 6543–6548; c) J. Rieger, T. Antoun, S. H. Lee, M. Chenal, G. Pembouong, J. L. de La Haye, I. Azcarate, B. Hasenknopf, E. Lacôte, *Chem. Eur. J.* **2012**, *18*, 3355–3361; d) M. B. Hu, N. Xia, W. Yu, C. Ma, J. Tang, Z. Y. Hou, P. Zheng, W. Wang, *Polym. Chem.* **2012**, *3*, 617–620; e) W.-K. Miao, Y.-K. Yan, X.-L. Wang, Y. Xiao, L.-J. Ren, P. Zheng, C.-H. Wang, L.-X. Ren, W. Wang, *ACS Macro Lett.* **2014**, *3*, 211–215; f) J. L. de La Haye, P. Beaunier, L. Ruhlmann, B. Hasenknopf, E. Lacôte, J. Rieger, *ChemPlusChem* **2014**, *79*, 250–256; g) J. Tang, W. Yu, M.-B. Hu, Y. Xiao, X.-G. Wang, L.-J. Ren, P. Zheng, W. Zhu, Y. Chen, W. Wang, *ChemPlusChem* **2014**, *79*, 1455–1462.

[9] a) J. Chen, L. M. Ai, W. Feng, D. Q. Xiong, Y. Liu, W. M. Cai, *Mater. Lett.* **2007**, *61*, 5247–5249; b) S. Shanmugam, B. Viswanathan, T. K. Varadarajan, *Nanoscale Res. Lett.* **2007**, *2*, 175–183; c) Z. L. Wang, Y. Ma, R. L.

Zhang, A. D. Peng, Q. Liao, Z. W. Cao, *Adv. Mater.* **2009**, *21*, 1737 – 1741; d) R. Yin, X. H. Guan, J. Gong, L. Y. Qu, *J. Appl. Polym. Sci.* **2007**, *106*, 1677 – 1682; e) X. F. Lu, X. C. Liu, L. F. Wang, W. J. Zhang, C. Wang, *Nanotechnology* **2006**, *17*, 3048 – 3053; f) N. Glezos, P. Argitis, D. Velessiotis, C. D. Diakoumakos, *Appl. Phys. Lett.* **2003**, *83*, 488; g) G. Zukowska, J. R. Stevens, K. R. Jeffrey, *Electrochim. Acta* **2003**, *48*, 2157 – 2164; h) D. G. Kurth, P. Lehmann, D. Volkmer, H. Colfen, M. J. Koop, A. Muller, *Chem. Eur. J.* **2000**, *6*, 385 – 393; i) H. L. Li, H. Sun, W. Qi, M. Xu, L. Wu, *Angew. Chem. Int. Ed.* **2007**, *46*, 1300 – 1303; *Angew. Chem.* **2007**, *119*, 1322 – 1325; j) H. Sun, H. L. Li, L. X. Wu, *Polymer* **2009**, *50*, 2113 – 2122.

[10] a) Y. Lan, E. B. Wang, Y. H. Song, Y. L. Song, Z. H. Kang, L. Xu, *Polymer* **2006**, *47*, 1480 – 1485; b) T. F. Otero, S. A. Cheng, E. Coronado, E. M. Ferrero, J. G. Carlos, *ChemPhysChem* **2002**, *3*, 808 – 811; c) H. L. Li, W. Qi, W. Li, H. Sun, W. F. Bu, L. X. Wu, *Adv. Mater.* **2005**, *17*, 2688 – 2692.

[11] a) A. Haimov, R. Neumann, *J. Am. Chem. Soc.* **2006**, *128*, 15697 – 15700; b) X. K. Lin, Y. L. Wang, L. X. Wu, *Langmuir* **2009**, *25*, 6081 – 6087; c) B. Wang, R. Vyas, S. Shaik, *Langmuir* **2007**, *23*, 11120 – 11126; d) Y. Nagaoka, S. Shiratori, Y. Einaga, *Chem. Mater.* **2008**, *20*, 4004 – 4010; e) L. Cheng, L. Niu, J. Gong, S. J. Dong, *Chem. Mater.* **1999**, *11*, 1465 – 1475; f) S. Q. Liu, H. Mohwald, D. Volkmer, D. G. Kurth, *Langmuir* **2006**, *22*, 1949 – 1951; g) S. Q. Liu, D. G. Kurth, H. Mohwald, D. Volkmer, *Adv. Mater.* **2002**, *14*, 225 – 228; h) L. Gao, E. B. Wang, Z. H. Kang, Y. L. Song, B. D. Mao, L. J. Xu, *Phys. Chem. B* **2005**, *109*, 16587 – 16592; i) P. J. Kulesza, M. Chojak, K. Karnicka, K. Miecznikowski, B. Palys, A. Lewera, A. Wieckowski, *Chem. Mater.* **2004**, *16*, 4128 – 4134.

[12] a) Z. Peng, *Angew. Chem. Int. Ed.* **2004**, *43*, 930 – 935; *Angew. Chem.* **2004**, *116*, 948 – 953; b) A. K. Cuentas-Gallegos, M. Lira-Cant'u, N. Casan-Pastor, P. Gomez-Romero, *Adv. Funct. Mater.* **2005**, *15*, 1125 – 1133;c) M. Carraro, M. Gardan, G. Scorrano, E. Drioli, E. Fontananova, M. Bonchio, *Chem. Commun.* **2006**, 4533 – 4535; d) M. Bonchio, M. Carraro, M. Gardan, G. Scorrano, E. Drioli, E. Fontananova, *Top. Catal.* **2006**, *40*, 133 – 140; e) M. Carraro, M. Gardan, L. Donato, G. Scorrano, E. Drioli, E. Fontananova, M. Bonchio, *Desalination* **2006**, *200*, 705 – 707;f) G. Gelbard, F. Breton, M. Quenard, D. C. Sherrington, *J. Mol. Catal. A* **2000**, *153*, 7 – 18; g) S. P. Das, J. J. Boruah, N. Sharma, N. S. Islam, *J. Mol. Catal. A* **2012**, *356*, 36 – 45.

[13] a) V. Singh, V. S. V. Satyanarayana, S. K. Sharma, S. Ghosh, K. E. Gonsalves, *J. Mater. Chem. C* **2014**, *2*, 2118 – 2122; b) V. Singh, V. S. V. Satyanarayana, S. K. Sharma, S. Ghosh, K. E. Gonsalves, *SPIE Advanced Lithography* **2014**, 905106-905106-8; c) V. S. V. Satyanarayana, F. Kessler, V. Singh, F. R. Scheffer, D. E. Weibel, S. Ghosh, K. E. Gonsalves, *ACS Appl. Mater. Interfaces* **2014**, *6*, 4223 – 4232.

[14] a) K. E. Gonsalves, J. Wang, H. J. Wu, *J. Vac. Sci. Technol. B* **2000**, 18, 325 – 327; b) G. M. Schmid, M. D. Stewart, J. Wetzel, F. Palmieri, J. J. Hao, Y. Nishimura, K. Jen, E. K. Kim, D. J. Resnick, J. A. Liddle, C. G. Willson, *J. Vac. Sci. Technol. B* **2006**, *24*, 1283 – 1291; c) B. K. Lee, N. G. Cha, L. Y. Hong, D. P. Kim, H. Tanaka, H. Y. Lee, T. Kawai, *Langmuir* **2010**, *26*, 14915 – 14922; d) H. W. Ro, V. Popova, L. Chen, A. M. Forster, Y. F. Ding, K. J. Alvine, D. J. Krug, R. M. Laine, C. L. Soles, *Adv. Mater.* **2011**, *23*, 414 – 420.

[15] a) M. Krysak, M. Trikeriotis, E. Schwartz, N. Lafferty, P. Xie, *Proc. SPIE.* **2011**, *7972*, XXVIII, 79721 C; b) M. Trikeriotis, W. J. Bae, E. Schwartz, M. Krysak, N. Lafferty, *Proc. SPIE.* **2010**, *7639*, XXVII, 76390 E.

[16] R. G. Finke, B. Rapko, R. J. Saxton, P. J. Domaille, *J. Am. Chem. Soc.* **1986**, *108*, 2947 – 2960.

[17] a) R. Neumann, A. M. Khenkin, *Chem. Commun.* **2006**, 2529 – 2538; b) R. Neumann, *Inorg. Chem.* **2010**, *49*, 3594 – 3601; c) K. Bineta, I. M. Mbomekalle, L. Nadjo, P. de Oliveira, A. Ranjbari, R. Contant, *C.R. Chimie* **2005**, *8*, 1057 – 1066.

[18] A. Corma, S. Iborra, F. X. Llabrés i Xamena, R. Monton, J. J. Calvino, C. Prestipino, *J. Phys. Chem. C* **2010**, *114*, 8828 – 8836.

[19] a) Y. Hou, C. L. Hill, *J. Am. Chem. Soc.* **1993**, *115*, 11823 – 11830; b) H. Zeng, G. R. Newkome, C. L. Hill, *Angew. Chem. Int. Ed.* **2000**, *39*, 1771 – 1774; *Angew. Chem.* **2000**, *112*, 1841 – 1844; c) C. P. Pradeep, D.-L. Long, G. N. Newton, Y. F. Song, L. Cronin, *Angew. Chem. Int. Ed.* **2008**, *47*, 4388 – 4391; *Angew. Chem.* **2008**, *120*, 4460 – 4463; d) C. P. Pradeep, F.-Y. Li, C. Lydon, H. N. Miras, D.-L. Long, L. Xu, L. Cronin, *Chem. Eur. J.* **2011**, *17*, 7472 – 7479; e) C. P. Pradeep, M. F. Misdrahi, F.-Y. Li, J. Zhang, L. Xu, D.-L. Long, T. Liu, L. Cronin, *Angew. Chem. Int. Ed.* **2009**, *48*, 8309 – 8313; *Angew. Chem.* **2009**, *121*, 8459 – 8463.

[20] a) K. Hakouk, O. Oms, A. Dolbecq, H. El Moll, J. Marrot, M. Evain, F. Molton, C. Duboc, P. Deniard, S. Jobic, P. Mialane, R. Dessapt, *Inorg. Chem.* **2013**, *52*, 555 – 557; b) H. El Moll, W. Zhu, E. Oldfield, L. Marleny Rodriguez Albelo, P. Mialane, J. Marrot, N. Vila, I. M. Mbomekalle, E. Riviere, C. Duboc, A. Dolbecq, *Inorg. Chem.* **2012**, *51*, 7921 – 7931.

[21] D. Li, H. Li, L. Wu, *Polym. Chem.* **2014**, *5*, 1930 – 1937.

[22] Bruker, SADABS, SMART, SAINTPLUS and SHELXTL, Bruker AXS Inc., Madison, WI, USA, **2000**.

[23] G. M. Sheldrick, SHELX-97, Program for Crystal Structure Solution and Refinement, University of Göttingen, Germany, **1997**.

Received: September 23, 2014
Published online on November 27, 2014

